Measurements of Oxygen Ion Spectra for Estimation of Electric Field Profiles in Cylindrical Plasmas

Takayuki KOBAYASHI, Masayuki YOSHIKAWA, Yuusuke KUBOTA, Ken MATAMA, Masamitsu NOTO, Junichi YOKOSHIMA and Teruji CHO

Plasma Research Center, University of Tsukuba, Tsukuba 305-8577, Japan

(Received 4 December 2006 / Accepted 20 March 2007)

Electric field profiles play an important role in the improvement of plasma confinement. It is essential to develop techniques to measure the electric field profiles in each region of a fusion device. We have developed a technique to measure the electric field profiles in cylindrical plasmas by measuring the Doppler shift of the CII spectrum. Recently, we have developed a collisional-radiative model for the lower charge state of oxygen ions. The oxygen emissions are stronger than those of carbon in GAMMA 10. In order to achieve a higher resolution for the electric field measurements, the technique for measuring the electric field profiles was improved by using the measurements of the oxygen spectra and the calculation of the newly developed collisional-radiative model. The electric field profile was successfully obtained under the condition of a weak electric field.

Keywords: electric field profile, spectroscopy, collisional-radiative model, cylindrical plasma, GAMMA 10

DOI: 10.1585/pfr.2.S1058

1. Introduction

Electric field profiles play an important role in the improvement of plasma confinement in fusion plasmas. In torus plasmas such as tokamak and helical systems, an H-mode and an internal transport barrier are associated with the electric field profiles [1, 2]. In tandem mirror systems, the electric field profiles play a similar role [3, 4]. Mirror devices having open-ended regions provide intrinsic important advantages in terms of the control of the radial potential or the sheared $\boldsymbol{E} \times \boldsymbol{B}$ rotation profiles on the basis of the axial particle-loss control. In order to study the physical basis for the improvement in plasma confinement, measurements of the electric field profiles in various plasmas are essential. We have developed a technique for measuring the electric field profiles by using an ultraviolet/visible (UV/V) spectroscopy and a collisional-radiative model (CR model) in cylindrical plasmas [5, 6]. The CR model was used for estimating the diamagnetic drift via the evaluation of an impurity density profile. In that study, the CII spectrum (426.726 nm: $2\,s^2 3d(^2D)$-$2\,s^2 4f(^2F)$) was observed, since the CR model calculation code for carbon ions has already been developed [7, 8]. However, the CII emission had a very low intensity even if the spectroscopic system had the maximum sensitivity in a wavelength region around 430 nm in the GAMMA 10 tandem mirror. The next goal of our study is continuous measurement in a typical plasma discharge, which is called hot-ion mode, with and without applying electron cyclotron resonance heating (ECRH) in the plug regions. The ECRH creates a strong electric field and electric field shear in the plug regions. The electric field is weak in an operation sequence without applying plug-ECRH. In this case, a higher resolution for the electric field measurement is required. The spectra of the oxygen ions (OII, OIII, OIV, and OV) have a high intensity in the UV/V wavelength region in the GAMMA 10 central cell and anchor cells. A CR model calculation code did not exist for the lower charge states of oxygen ions that is applicable to the study of impurities in GAMMA 10. Recently, we began developing the CR model for oxygen ions for GAMMA 10 plasma measurements. We evaluated the density profile of oxygen ions by using our new code [9, 10]. Moreover, the CCD camera system was revised to achieve a higher wavelength resolution than that of the previous system. In this paper, we show the results of the electric field profile measured by using the new spectroscopic system and the newly constructed CR model for oxygen ions in order to achieve a higher resolution for the electric field measurements.

2. Principle of Measurements

We have developed a technique for measuring the electric field profiles in cylindrical plasmas. In this technique, we measure the Doppler shift ($\Delta\lambda$) of an impurity spectrum, which depends on the rotation velocity of the impurity. The rotation velocity ($u_\perp$) of the cylindrical plasma depends on the $\boldsymbol{E} \times \boldsymbol{B}$ drift velocity and the diamagnetic drift velocity as follows:

$$\Delta\lambda = \lambda_0 \frac{v_1}{c}, \tag{1}$$

$$u_\perp = \frac{\boldsymbol{E} \times \boldsymbol{B}}{B^2} - \frac{\nabla p \times \boldsymbol{B}}{Zen_z B^2}, \tag{2}$$

author's e-mail: tkobaya@prc.tsukuba.ac.jp

where λ_0, c, B, and e are the wavelength of the spectrum, speed of light, magnetic field strength, and electron charge, respectively. Z, p, and n_z are the charge number, pressure, and density of the impurity, respectively. The first term in Eq. (2) is the $\boldsymbol{E} \times \boldsymbol{B}$ drift velocity and the second one is the diamagnetic drift velocity. Further, we obtained an emission profile of the impurity spectrum. The emissivity (I_{ij}^z) is proportional to the electron density (n_e) and the impurity density (n_z) as follows:

$$I_{ij}^z = R_{ij}^z n_e n_z, \tag{3}$$

where R_{ij}^z is an effective emission rate coefficient that is calculated using the CR model. Therefore, we can obtain the impurity density profile by using Eq. (3). The diamagnetic drift velocity is calculated using the impurity density and temperature, which is evaluated by the Doppler broadening of the spectrum. In principle, by using the above procedure, we can obtain the electric field under the condition that the magnetic field strength is known. The observed spectra are line-integrated signals. Then, we developed a technique for numerical analysis called the parametric Abel inversion technique, which is described in Ref. 3.

3. Spectroscopic System

In GAMMA 10, two UV/V spectroscopic systems are installed on the south side of the central cell mid plane and the top side of the west anchor cell. Recently, we revised the CCD camera system in the central cell system such that it achieves a higher wavelength resolution than that of the previous one. Figure 1 shows a schematic view of the newly constructed UV/V spectroscopic system in the central cell. The system views the plasma column vertically. The impurity emission from a cylindrical plasma in the central cell region is collected by quartz lenses and is transferred to a spectrometer through an 8-m-long bundled optical fiber array. Each optical fiber comprises a quartz core with a diameter of 400 μm. The light collection system covers the range from $x = -20$ cm to $x = 20$ cm with a channel separation of 1 cm. The optical fibers are connected to the entrance slit (50 μm) of a 1-m-long Czerny-Turner spectrometer with a grating of 2400 grooves/mm. The observable wavelength is in the range from 200-700 nm. The upper limit is determined by the spectrometer grating and the lower limit is determined by the transmission of the quartz fiber. At the exit plane, the light from each fiber provides the spectrum of each spatial position. The image of the exit plane is focused onto an image intensifier tube (Hamamatsu 4435U) and then the spectrum is exposed by the CCD camera (QImaging Retiga 1300R cooled-type) with lens coupling. The maximum frame rate is 50 fps with 10 ms exposure time. The output of the CCD camera is transferred to a personal computer and is stored as a 12-bit-depth TIFF file image. The relative sensitivity, wavelength resolution, and dispersion in the CCD image are calibrated using a 1.2-m-long linear mercury lamp. At $\lambda = 312.6$ nm, the wavelength resolution and dispersion are 0.03 nm and 0.006 nm/pixel, respectively. The resolutions are approximately two times higher than those of the previous CCD camera system. These calibration results are shown in Fig. 2.

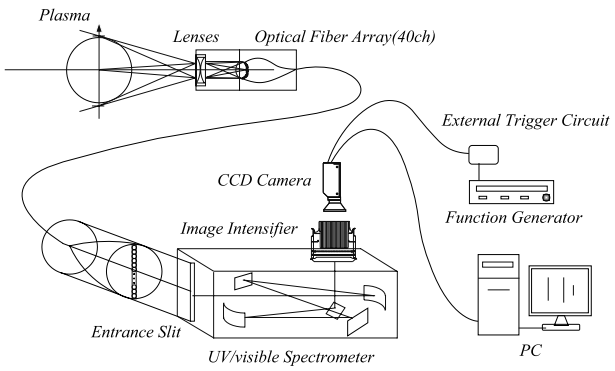

Fig. 1 Schematic view of UV/V spectroscopic system in the central cell.

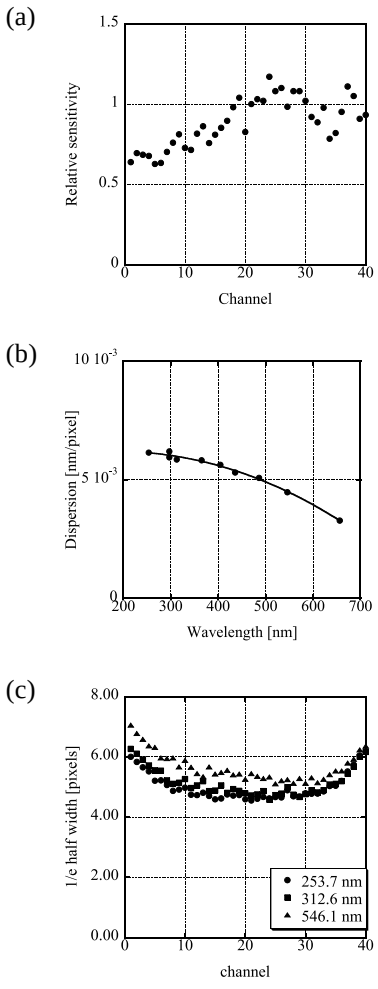

Fig. 2 Calibration results of UV/V spectroscopic system with revised CCD camera, (a) relative sensitivity, (b) wavelength dispersion and (c) wavelength resolution.

4. Experimental Results and Analyses

In the central cell of GAMMA 10, the highest emissions from the oxygen ions OII, OIII, OIV, and OV are 441.5 nm, 298.3 nm, 306.3 nm, and 278.1 nm, respectively. The configurations of the levels and transition rates are listed in Table. 1. In order to select the most useful spectrum for evaluating the electric field profiles, we measured these spectra in the hot-ion mode and compared their emission profiles. Figure 3 shows the normalized emissivity profiles of these spectra obtained by the Abel inversion. From the viewpoint of the electric field measurements, the OIII emission was the most useful spectrum because its emission profile was the broadest. Therefore, the OIII emission includes the widest spatial information of the electric field profiles. In addition, the O^{2+} ion temperature was not so high according to a measurement of the Doppler broadening. Therefore, an effect of the $\boldsymbol{E} \times \boldsymbol{B}$ drift velocity should be clearly observed in the Doppler shift measurements. We used OIII emission for the electric field profile measurements in this study. Figure 4 shows (a) a measurement result of the OIII brightness profile (closed circle) and (b) an emissivity profile obtained by the Abel inversion. The result of the reconstruction from the emissivity to the line integrated intensity is denoted in Fig. 4 (a) by a solid line. We evaluated the O^{2+} density profile using the CR model and its result is shown in Fig. 5. In this case, the O^{2+} ion temperature was approximately 300 eV, which was obtained from the Doppler broadening. Therefore, we obtained the diamagnetic drift velocity of O^{2+}, which is denoted in Fig. 6 by a broken line. We applied the parametric Abel inversion technique to this result. Figure 7 shows the Doppler shift profiles that were obtained by the measurement of the line-integrated spectrum (closed circle) and the best-fitted calculation result of the parametric Abel inversion (solid line). This result indicates that the electric field profile in the central cell of GAMMA 10 is as shown in Fig 8. In this case, the rotation velocity owing to the $E \times B$ drift and the total rotation velocity are denoted by the dotted line and solid line, respectively, in Fig. 6. The measurement result of the Doppler shift had a statistical error. In the previous study described in Ref. 3, which used the old CCD camera system and CII emission, the error was approximately 0.006 nm. In this study, it was approximately 0.003 nm. The maximum error in the measured electric field was improved from ±1000 V/m to ±500 V/m. There-

Table 1 The table of spectral information, wavelength (wl), configuration of final state (Final), configuration of initial states (Initial) and the transition Probability (Aij).

	wl	Final	Initial	Aij
OII	441.5	$2s^22p^2(^3P)3s(^2P)_{3/2}$	$2s^22p^2(^3P)3s(^2D^0)_{5/2}$	7.16e+7
OIII	298.3	$2s^22p^2(^2P^0)3s(^1P^0)_1$	$2s^22p^2(^2P^0)3s(^1P^0)_2$	2.15e+8
OIV	306.3	$2s^23s(^2S)_{1/2}$	$2s^23p(^2S)_{3/2}$	1.30e+8
Ov	278.1	$1s^22s3s(^3S)_1$	$1s^22s3p(^3P^0)_2$	1.40e+8

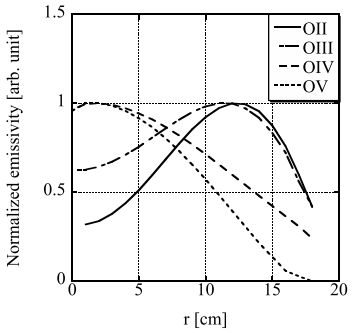

Fig. 3 Normalized emissivity profiles of oxygen spectra.

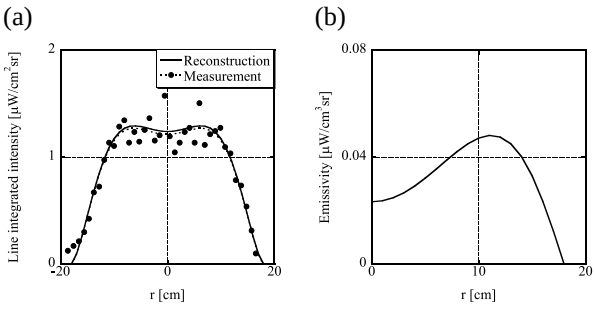

Fig. 4 (a) Measurement result (closed circle) of the line integrated OIII emission intensity and the result of reconstruction after Abel inversion (solid line). (b) The emissivity profile of OIII obtained by Abel inversion.

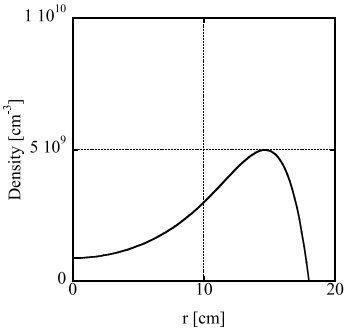

Fig. 5 The density profile of O^{2+} ion.

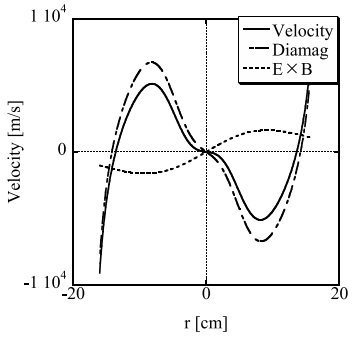

Fig. 6 Total velocity (solid line), diamagnetic drift velocity (broken line) and $E \times B$ drift velocity (dotted line).

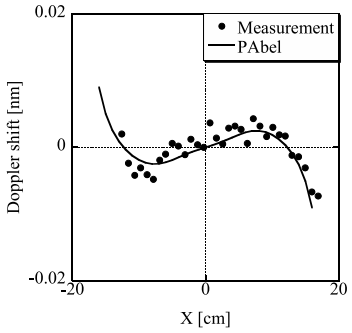

Fig. 7 The result of the Doppler shift measurement (open circle) and the best fitted result of the parametric Abel inversion (solid line).

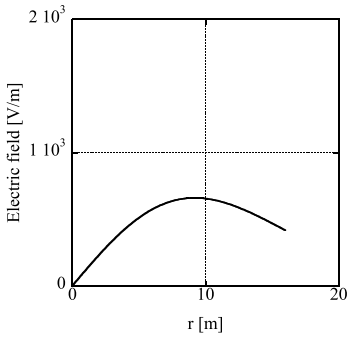

Fig. 8 Obtained result of the electric field profile by the parametric Abel inversion.

fore, we successfully obtained the electric field profile in the discharged condition of the weak electric field, without plug-ECRH, in the central cell of GAMMA 10. We will attempt to continuously measure the electric field profiles in the central cell and discuss the plasma confinement in various plasma discharge sequences. Moreover, we have attempted to evaluate the electric field profile in the west anchor cell. In this region, the electric field profile is expected to be the same as that in the central cell; however, this has not yet been measured.

5. Conclusion

In order to evaluate the electric field profile in various plasma discharge sequences, we revised the CCD camera system of the UV/V spectroscopic system. Moreover, we developed a new CR model for the lower charge state of oxygen ions. Therefore, the electric field profile was successfully obtained under the condition of a weak electric field in the central cell of GAMMA 10.

Acknowledgements

The authors would like to thank members of GAMMA 10 group of the University of Tsukuba for their collaboration. This work was partly supported by Ministry of Education, Culture, Sports, Science and Technology, Grant-in-Aid for Scientific Research in Priority Areas, No. 16082203.

[1] J.W. Connor *et al.*, Plasma Phys. Control. Fusion **42**, R1 (2000).
[2] P.H. Diamond *et al.*, Plasma Phys. Control. Fusion **47**, R35 (2005).
[3] T. Cho *et al.*, Phys. Rev. Lett. **94**, 085002 (2005).
[4] T. Cho *et al.*, Phys. Rev. Lett. **97**, 055001 (2006).
[5] T. Kobayashi *et al.*, Rev. Sci. Instrum. **75**, 4121 (2004).
[6] M. Yoshikawa *et al.*, Trans. Fusion Technol. **39**, 289 (2001).
[7] T. Kato *et al.*, Fusion Eng. Des. **34-35**, 789 (1997).
[8] M. Yoshikawa *et al.*, J. Plasma Fusion Res. SERIES **6**, 685 (2004).
[9] T. Kobayashi *et al., Proc. of 33rd EPS, Conference on Plasma Physics* (2006).
[10] T. Kobayashi *et al.*, Trans. Fusion Technol. **51**, 256 (2007).